FFDM Software Development Series 1

Introduction to SLOPE-DISP 3.0

Ching-Chuan Huang

Professor Emeritus
Department of Civil Engineering,
National Cheng Kung University, Tainan, Taiwan
Email: samhcc@mail.ncku.edu.tw
2024/10/02

1.1 BACKGROUND

Designs and analyses for soil structures using limit equilibrium methods (LEM) have been conducted as engineering practices for more than 200 years. Results of slope stability analyses using limit equilibrium methods are represented by the safety factor (F_s) of the slope, defined as the ratio between the shear strength and the shear stress of the material that forms the slip surface. Although the value of F_s has long been used as an indicator for the slope stability status, it has intrinsic shortcomings that hinder insightful slope stability designs and analyses: (1) Displacements of the slope and/or shear displacements along the slip surface are unknown; (2) The definition of F_s is based on a major assumption, i.e., a unique F_s along the slip surface. Therefore, the value of F_s is somewhat a 'semi-quantitative' indicator, rather than a quantitative one. The judgement on the safety status of the slope based on values of F_s is neither straightforward nor accurate and is largely dependent on empiricism.

To remediate the above shortcomings of LEM-based slope stability analysis, a Force-equilibrium-based Finite Displacement Method (FFDM) is developed (Huang, 2013). In the FFDM, the Fellenius' method, the Bishop's method, the Janbu's method, the Spencer's method and the multi-wedge method are modified to accommodate the new theory. In this report (FFDM Software Development Series 1), features of FFDM including its advantages and disadvantages are highlighted. In addition, three essential components that constitute the framework of FFDM are also introduced in Sections 1.4 through 1.6. These fundamental components include: (1) Stress-displacement constitutive law of soils; (2) Force and/or moment equilibrium for the entire sliding mass.; (3) Displacement compatibility of sliding soil mass.

1.2 ADVANTAGES OF FFDM

The FFDM for reinforced slopes has the following features that are distinct from the existing stability analysis methods:

(1) Providing a vertical settlement at the crest as well as shear displacements along the critical failure surface of the analyzed slope. A vertical settlement of the slope is often deemed as an important displacement-based indicator of the slope.

(2) Providing local displacement-based and stress-based safety factors along the failure surface instead of a lumped safety factor for the entire slip surface.

(3) Providing slope displacements with little additional time and effort, as compared to conventional slope stability methods. The computer time needed in calculating slope displacements using non-linear (hyperbolic) stress-displacement relationships constitutive laws is no more than that needed in a conventional limit equilibrium calculation for a constant value of safety factor.

(4) The shear stress-displacement relationship in FFDM is like that used in the discrete element method (DEM) in which stress-displacement relationships are used to obtain normal and shear spring constants under small displacement conditions, except that the stress-displacement relationship used in FFDM covers relatively large shear displacement conditions.

(5) Adopting the notion of incremental slope displacements or cumulative slope displacements between two different internal and/or external loading states.

(6) FFDM is equally applicable to unreinforced and reinforced slopes. In the case of reinforced slopes, the mobilized reinforcement force is a part of analytical output. This is not the case in conventional LEM-based analyses.

1.3 LIMITATIONS OF FFDM

The FFDM has the following limitations:

(1) Potential failure surfaces must be prescribed in the FFDM analysis as in conventional LEM analyses. Possible shapes of failure surfaces include straight lines, bi-linear wedges, multi-wedges, circles, logarithmic spirals, and a combination of the above-mentioned ones. A group of potential failure surfaces are used in a trial-and-error manner to search for a critical surface associated with a maximum slope displacement in the FFDM analysis.

(2) Slope displacements can be calculated at the cost of three more input soil parameters required by the hyperbolic stress-displacement constitutive law. They are the initial shear stiffness number (K), the stress-dependency exponent (n) and the peak-to-asymptote strength ratio (R_f). These parameters can be obtained via calibrations of the slope displacements during the initial phase of field monitoring, direct shear tests, or empirical equations.

1.4 STRESS-DISPLACEMENT CONSTITUTIVE LAW

The following hyperbolic equation as schematically shown in Fig. 1.4.1 is used for the normalized shear stress (τ/τ_f) vs. shear displacement (Δ) relationship along the potential failure surface (Duncan and Chang, 1970; Huang, 2013):

$$\frac{\tau}{\tau_f} = \frac{\Delta}{a + b \cdot \Delta} \qquad (1-4-1)$$

$$a = \frac{\tau_f}{k_{initial}} \qquad (1-4-2)$$

$$b = R_f \qquad (1-4-3)$$

$$R_f = \frac{\tau_f}{\tau_{ult}} \qquad (1-4-4)$$

$k_{initial}$: initial shear stiffness of soils

τ_{ult}: asymptote strength at infinite displacement

τ_f:: shear strength of soil based on Mohr-Coulomb failure criterion

R_f: asymptote strength ratio (= τ_f / τ_{ult})

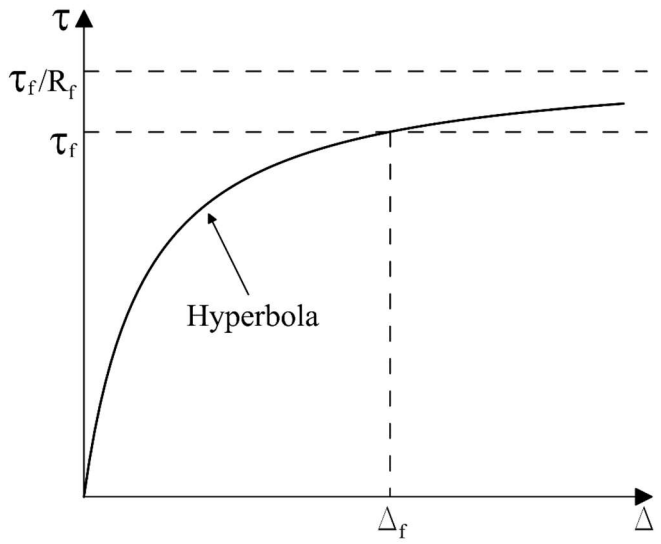

Figure 1.4.1 A hyperbolic normalized stress and shear displacement relationship

The shear strength of soils (τ_f) is described based on Mohr-Coulomb failure criterion:

$$\tau_f = c + \sigma_n' \cdot \tan\varphi \qquad (1-4-5)$$

σ_n': Effective normal pressures

c: cohesion intercept

φ: Internal friction angle of soils

Note that Eq. (1-4-1) is the inverse of local safety factor F_s at the base of a slice

(or a soil wedge):

$$F_s = \frac{\tau_f}{\tau} \qquad (1-4-6)$$

The initial shear stiffness can be expressed as a power function (Duncan and Chang, 1970) of effective normal pressure (σ_n') on the failure surface:

$$k_{initial} = K \cdot G \left(\frac{\sigma'_n}{P_a} \right)^n \qquad (1-4-7)$$

K: initial shear stiffness number (a non-dimensional material constant)

P_a: atmospheric pressure (= 101.3 kPa)

G: reference shear stiffness (= 101.3 kPa/m)

n: pressure dependency exponent

The stress-displacement constitutive law expressed by Eqs. 1-4-1 through 1-4-7 are substantiated by a study on various types of soils based on medium-to-large scale direct shear test results and a curve-fitting technique. Details of the tests and curve-fitting will be reported in a forthcoming series of reports.

1.5 FORCE AND MOMENT EQUILIBRIA

This section briefly describes force and moment equilibria considered various types of analyses. Details of formulations will be given in a forthcoming series of reports. Three types of force and moment equilibrium are adopted in slope stability formulations for a potential sliding mass with slices:

1. For a circular failure surface as shown in Fig. 1.5.1, Fellenius' method (Fellenius, 1936), and Bishop's method (Bishop, 1955) fall in this category. In these methods, the vertical (or normal to
   the slice base) force equilibrium and the over-all moment equilibrium of the circular sliding mass are formulated.

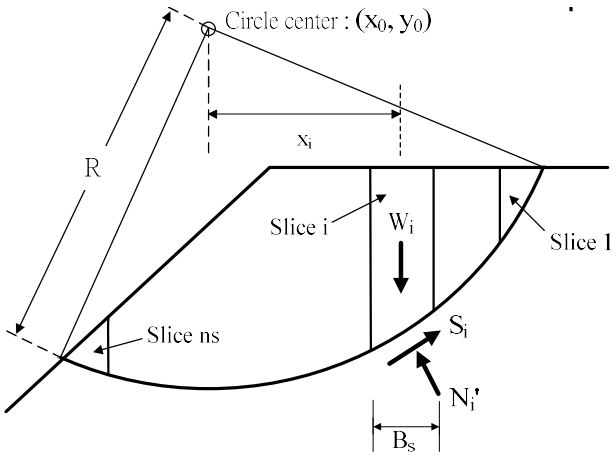

Fig. 1.5.1 A potential failure mass confined by a circular failure surface

2. For a non-circular failure surface as shown in Fig. 1.5.2, the rigorous Janbu's method (Janbu, 1973), and Spencer's method (Spencer, 1973) fall in this category. In these methods, force equilibrium (both in vertical and horizontal directions) and moment equilibrium for every slice in the sliding mass are formulated. In the simplified Janbu's method, however, only force equilibrium in vertical and horizontal directions are formulated.

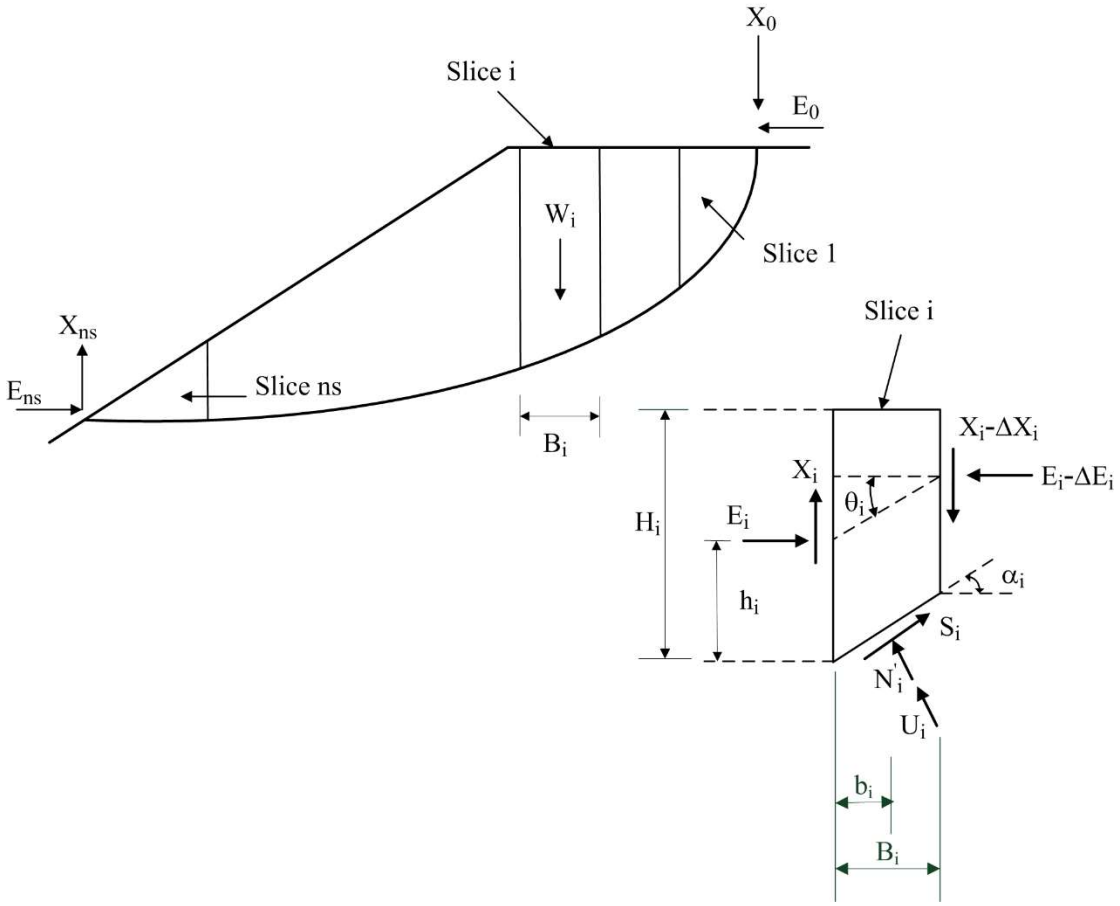

Fig. 1.5.2 Body and reactional forces in a sliced non-circular failure mass

3. For a wedge-like failure surface as shown in Fig. 1.5.3, the Multi-wedge method (Huang, et al., 2003) and the simplified Janbu's method fall in this category. In these methods, only force equilibrium in vertical and horizontal directions are formulated.

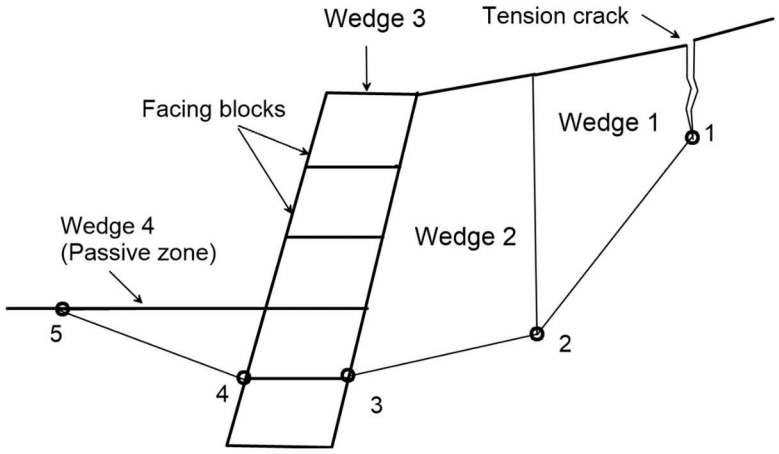

Fig. 1.5.3 Schematic wedge-like failure mass

1.6 DISPLACEMENT COMPATIBILITY

A hodograph (or displacement diagram) that satisfies displacement compatibility (Atkinson, 1981), schematically shown in Fig. 1.5.3(a) and 1.5.3(b), yields:

$$\Delta_2 = \Delta_1 \cdot \frac{\cos(\alpha_1 - 2\psi)}{\cos(2\psi - \alpha_2)} = \frac{\Delta_0}{\sin(\alpha_1 - \psi)} \cdot \frac{\cos(\alpha_1 - 2\psi)}{\cos(2\psi - \alpha_2)} \qquad (1-6-1)$$

where ψ is the angle of the dilatancy of soils.

For the case of i >3:

$$\Delta_i = \Delta_{i-1} \cdot \frac{\cos(\alpha_{i-1} - 2\psi)}{\cos(2\psi - \alpha_i)}$$

$$= \frac{\Delta_0}{\sin(\alpha_1 - \psi)} \cdot \frac{\cos(\alpha_1 - 2\psi)}{\cos(2\psi - \alpha_2)} \cdot \frac{\cos(\alpha_2 - 2\psi)}{\cos(2\psi - \alpha_3)} \cdots\cdots\cdots$$

$$\cdot \frac{\cos(\alpha_{i-1} - 2\psi)}{\cos(2\psi - \alpha_i)} \qquad (1-6-2)$$

Note that in Eq. (1-6-2),

$$\cos(2\psi - \alpha_2) = \cos(\alpha_2 - 2\psi) \qquad (1-6-3)$$

Therefore, a general expression for Δ_i is obtained as:

$$\Delta_i = \Delta_0 \cdot f(\alpha_i) \qquad (1-6-4)$$

$$f(\alpha_i) = \frac{1}{\sin(\alpha_1 - \psi)} \cdot \frac{\cos(\alpha_1 - 2\psi)}{\cos(2\psi - \alpha_i)} \qquad (1-6-5)$$

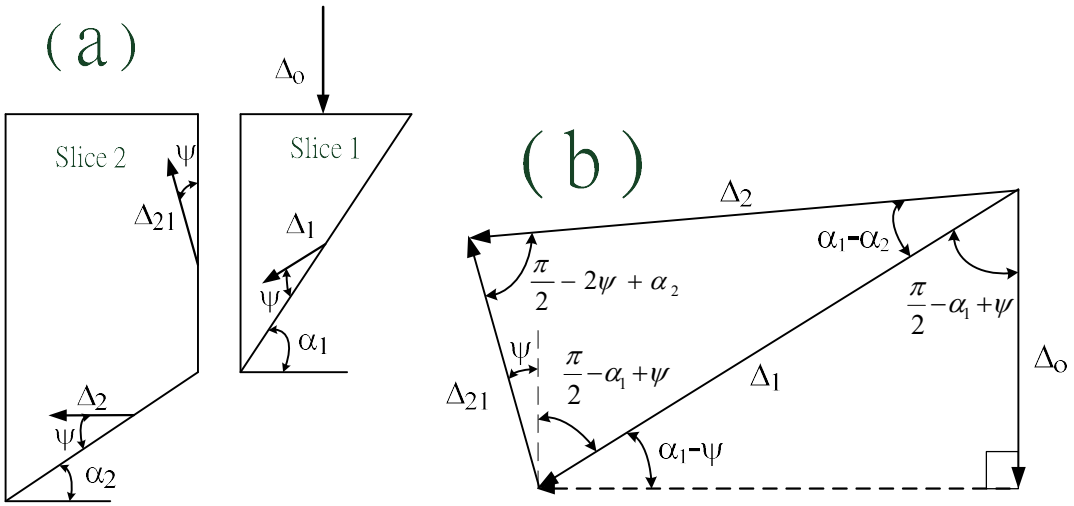

Fig. 1.6.1 Displacement compatibility of adjacent slices:

(a) vectors of shear displacement; (b) displacement diagram

Figure 1.6.2(a) schematically shows a potential sliding mass under a constant volume (i.e., an angle of dilatancy $\Psi = 0$) state. Vectors of shear displacements (Δ_1, ---, Δ_7) at the slice base and the slice interface are also shown. Displacement diagram (or Hodograph) for this case is shown in Fig. 1.6.2(b).

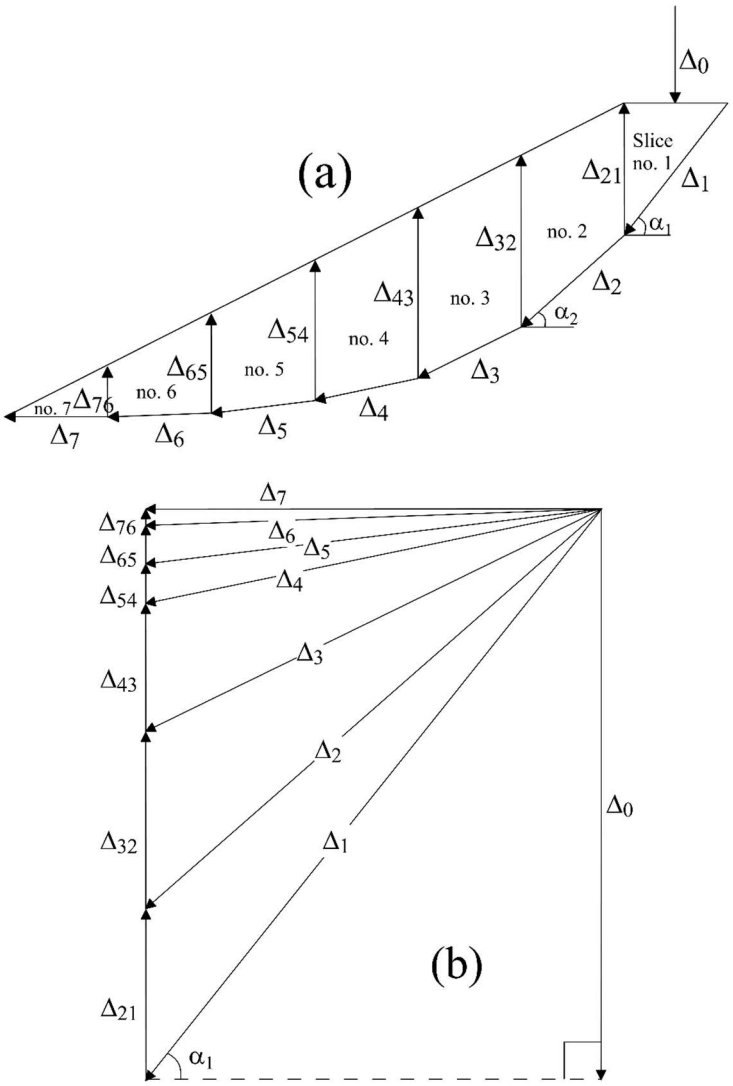

Figure 1.6.2 A constant-volume (Ψ=0) sliding mass with (a) Displacement vectors at the base of slice; (b) Hodograph of the sliding mass

Figure 1.6.3(a) schematically shows the case of dilative state of the sliding mass, namely $\Psi > 0$, the vector of shear displacement at the base of the slice has an angle of Ψ with the base of slice. A hodograph for the case of $\Psi > 0$ is shown in Fig. 1.6.3(b) which indicates that for a sliding mass under $\Psi > 0$ condition, shear displacements along the potential sliding surface increase towards the toe of the slope.

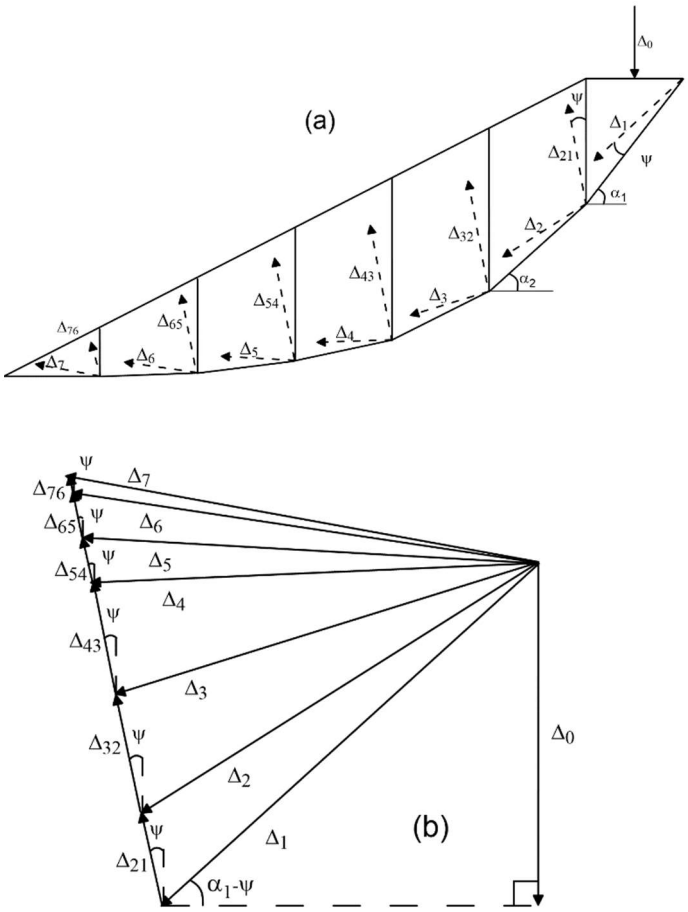

Figure 1.6.3 A constant-volume ($\Psi > 0$) sliding mass with (a) Displacement vectors at the base of slice; (b) Hodograph of the sliding mass

Figure 1.6.4(a) schematically shows the case of dilation (or expansion) of the sliding mass, namely $\Psi < 0$, the vector of shear displacement at the base of the slice has an angle of dilation (Ψ) with the base of slice. A hodograph for the case of $\Psi < 0$ is shown in Fig. 1.6.4(b).

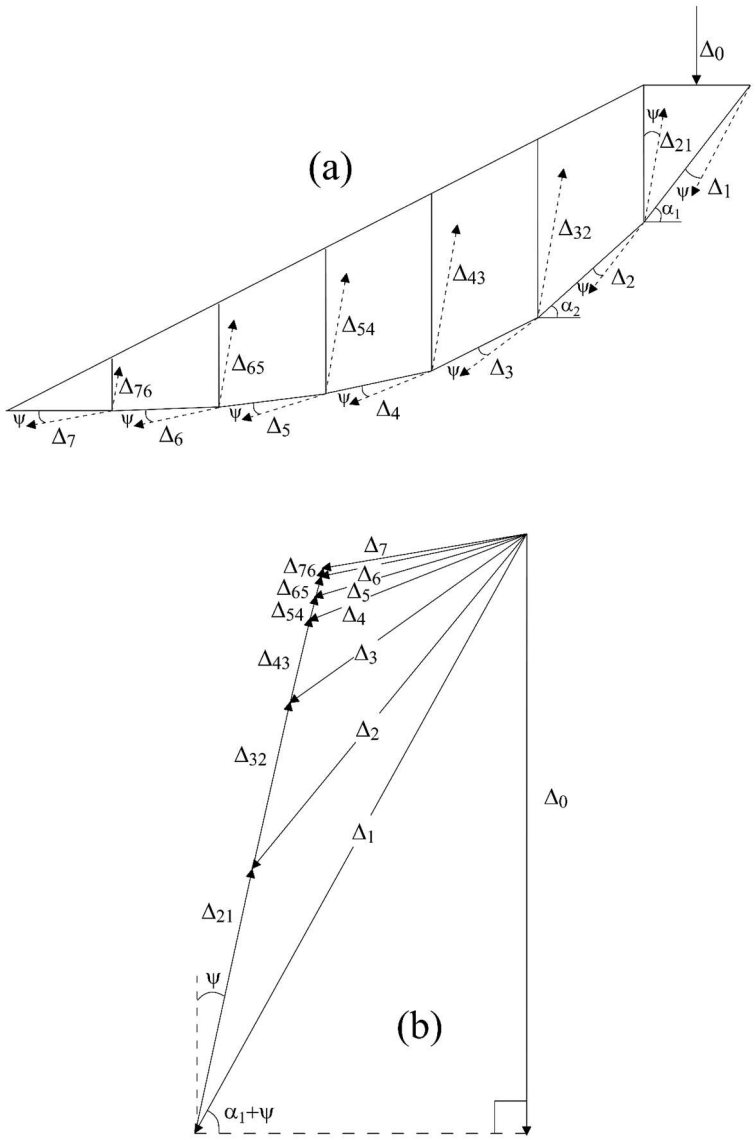

Figure 1.6.4 A constant-volume ($\Psi < 0$) sliding mass with (a) Displacement vectors at the base of slice; (b) Hodograph of the sliding mass

1.7 DISPLACEMENT INCREMENT

In calculating slope displacements induced by external and internal condition changes (e.g., loading, water table, or pore water pressure variations), two values of Δ_i, namely, a slope displacement prior to the event $\left(\Delta_i^a\right)$ and that after the event $\left(\Delta_i^b\right)$, can be calculated. The increment of displacement for slice *i*, induced by the stress change is schematically shown in Fig. 1.7.1, and is defined as:

$$\Delta_i = \Delta_i^b - \Delta_i^a \qquad (1-7-1)$$

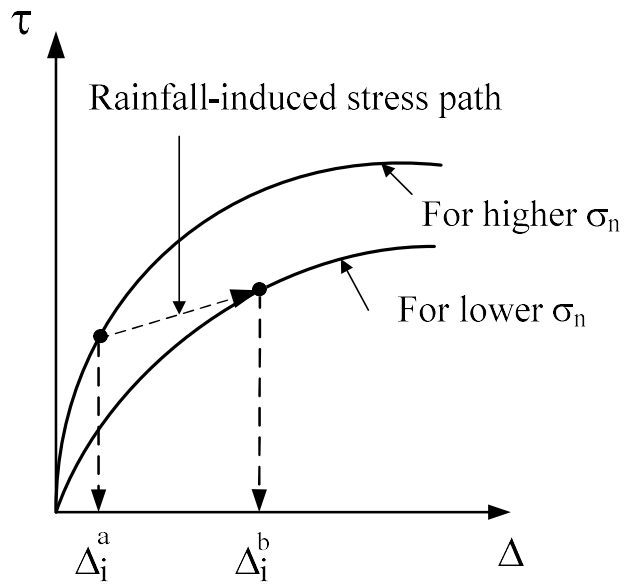

Fig. 1.7.1 Possible shear stress and displacement increases induced by a coupled shear and confining stress increases

REFERENCE

Atkinson, J.H. (1981) “An introduction to applications of critical state soil mechanics” McGraw-Hill, London.

Bishop, A.W. (1955) “The use of slip circle in the stability analysis of slopes” Geotechnique, Vol. 5, No. 1, pp. 7-17.

Duncan, J.M. and Chang, C.Y. (1970) “Nonlinear analysis of stress and strain in soils” Journal of the Soil Mechanics and Foundation Division, ASCE, Vol. 96, No. SM5, pp. 1629-1653.

Fellenius, W. (1936) “Calculation of the stability of earth dams” Proceedings of 2nd Congress on Large Dams, Vol. 4, pp. 445-463.

Huang, C.-C. (2013) “Developing a new slice method for slope displacement analyses” Engineering Geology, Vol. 157, pp. 39-47.

Huang, C.-C., Chou, L.H. and Tatsuoka, F. (2003) “Seismic displacements of geosynthetic-reinforced soil modular block walls” Geosynthetics International, Vol. 10, No. 1, pp. 2-23.

Janbu, N. (1973) Slope stability computation, Embankment-Dam Engineering, Casagrande Volume, John Wiley & Sons, pp. 47-86.

Spencer, E. (1973) “Thrust line criterion in embankment stability analysis” Geotechnique, Vol. 23, No. 1, pp. 85-100.